A Resiliency-oriented Optimal Operation of Microgrids Considering Electric Vehicles

A Resiliency-oriented Optimal Operation of Microgrids Considering Electric Vehicles

Seyed Farhad Zandrazavi
School of Technology and Innovations
University of Vaasa
Vaasa, Finland
seyed.zandrazavi@uwasa.fi

Alejandra Tabares
Department of Industrial Engineering
Los Andes University
Bogotá, Colombia
a.tabaresp@uniandes.edu.co

John Fredy Franco
Department of Electrical Engineering
São Paulo State University
Ilha Solteira, Brazil
j.f.franco@ieee.org

Miadreza Shafie-khah
School of Technology and Innovations
University of Vaasa
Vaasa, Finland
mshafiek@uwasa.fi

João Soares
GECAD, LASI, School of Engineering
Polytechnic of Porto
Porto, Portugal
jan@isep.ipp.pt

Zita Vale
GECAD, LASI, School of Engineering
Polytechnic of Porto
Porto, Portugal
zav@isep.ipp.pt

***Abstract*— The sharp increase in renewable energy generation and the number of electric vehicles enhance power systems' modernization, decarbonization, and decentralization. As a result, microgrids (MGs) with renewable energy integration and charging facilities have attracted significant attention. Nonetheless, disregarding uncertainties in optimization models for MGs can lead to either risky or costly decisions. In addition, sustainable development and operation of MGs must enhance the system's resiliency to guarantee functionality during abnormal situations. Therefore, this paper proposes a two-stage stochastic programming model to ensure the resilient operation of microgrids with charging facilities. At the same time, uncertainties associated with renewable generation, demand, and market price are addressed via scenarios. To enhance resiliency against unplanned islanding, a scenario for outages is defined so that preventive actions can be done in the first stage to robust the energy management of the microgrid.**

***Keywords*— Charging stations, microgrid, optimal operation, renewable energy, resiliency.**

I. INTRODUCTION

Previous studies have shown that a substantial reduction in greenhouse gas (GHG) emissions (between 50% and 80%) is required to achieve global climate targets by 2050 [1]. Renewable energy-based distributed generation and plug-in electric vehicles (EVs) can help to considerably decline GHG emissions [2]. To this end, due to their structures and characteristics, microgrids (MGs) can play an important role in energy transition by accommodating more clean distributed energy generation units and by supplying the required energy for new EVs, in both grid-connected and islanded modes. Furthermore, MGs can enhance the reliability, resiliency, sustainablity, and efficiency of modern power systems. A comprehensive review of the benefits of MGs for current and future energy systems can be found in [3].

This research was supported by the Brazilian institutions: Coordination for the Improvement of Higher Education Personnel (CAPES) - Finance Code 001, Brazilian National Council for Scientific and Technological Development (CNPq) under Grant 409359/2021-1, and the São Paulo Research Foundation (FAPESP), under grants 2015/21972-6, 2018/08008-4, 2022/03161-4, and Los Andes University. This article is a result of the project RETINA (NORTE-01-0145-FEDER-000062), supported by Norte Portugal Regional Operational Program (NORTE 2020), under the PORTUGAL 2020 Partnership Agreement, through the European Regional Development Fund (ERDF). The authors acknowledge the work facilities and equipment provided by GECAD research center (UIDB/00760/2020) to the project team. João Soares also acknowledges FCT for grant CEECIND/00420/2022. Seyed Farhad Zandrazavi also acknowledges Finnish Cultural Foundation for grant 00231255 Central Fund.

Despite their advantages, the optimal operation of MGs can be quite complicated since many different technical and economical constraints should be considered. Furthermore, uncertainties related to renewable generation, electric demand, and energy prices can profoundly affect the accuracy of the optimal solutions. As a result, the optimal operation of MGs has been studied widely in previous research and different methods for modeling uncertainties were proposed. For example, a framework for optimal scheduling of microgrids based on two-stage robust optimization was proposed in [4], while interval sets are defined for renewable generation, electricity price, and electric demand. However, EVs are not considered in that framework. In [5], a two-level optimization model for optimal scheduling of microgrids including heat pumps with thermal storages was proposed, yet uncertainties and power flow were not considered in the proposed model. A stochastic model for the optimal energy management of resilient MGs was proposed in [6], while the uncertainty of the voltage reference at the point of common coupling is considered; nevertheless, due to computational burden, the unplanned islanding scenarios (i.e., outage scenarios) are selected arbitrarily. Although numerous models have been proposed for the optimal operation of MGs in the literature, some of the previous works neglect power flow in the steady-state modeling of the electrical power systems. In addition, some studies did not include EVs or did not address the resiliency issue. To address that gap, a novel algorithm based on a two-stage stochastic model is proposed in this paper to not only enhance the resiliency of MGs against unplanned islanding but also incorporate power flow and uncertainties within the proposed model. Hence, the major contributions of this study can be summarized as:

- A mixed-integer second-order cone programming model for the two-stage stochastic optimal energy management of microgrids considering EV charging stations.
- Rescheduling microgrids to enhance its resiliency against unplanned outages when microgrids are more vulnerable and dependent on the main grid.

II. UNCERTAINTY MODELING

Well-suited probability density functions (PDFs) for modeling uncertainties associated with solar irradiation, wind speed, and electric demands are presented in this section. In addition, a set of scenarios is derived from the PDFs for each uncertain parameter. Furthermore, the generation of photovoltaic and wind turbine units are computed based on the respective scenarios of solar irradiance and wind speed.

A. Weibull PDF for Wind Speed

In this paper, Weibull PDF is used to model the uncertainty of wind speed. The shape of the Weibull density function can vary depending on the values of its two parameters, the scale and shape of the distribution. In general, the distribution tends to be skewed towards one end of the range or the other, with a decre asing hazard rate over time for values of one parameter and an increasing hazard rate for the other. The Weibull PDF for the variable y is presented in (1), where parameters k and c are shape and scale indices and their values are obtained based on (2). Additionally, parameters σ and μ are the standard deviation and expected value of the random variable y [7]. Furthermore, the relation between wind speed (S^{WT}) and the generation of WT units (P^{WT}) is presented in (3) and variables S_{co}^{WT}, S_{ci}^{WT}, and S_{no}^{WT} in (3) are cut-out, cut-in, and nominal speed, while variable P_{no}^{WT} represents nominal capacity [8].

$$PDF(y) = e^{-\left(\frac{y}{c}\right)^k}\frac{k}{c}\left(\frac{y}{c}\right)^{k-1} \tag{1}$$

$$k = 2,\ c = \frac{\mu}{\Gamma\left(1+\frac{1}{k}\right)} \tag{2}$$

$$P^{WT} = \begin{cases} 0 \quad if\ S_{co}^{WT} < S^{WT}\ or\ S^{WT} < S_{ci}^{WT} \\ P_{no}^{WT}\left(\dfrac{S^{WT} - S_{ci}^{WT}}{S_{no}^{WT} - S_{ci}^{WT}}\right)\ if\ S_{ci}^{WT} < S^{WT} \le S_{no}^{WT} \\ P_{no}^{WT} \quad if\ S_{no}^{WT} < S^{WT} \le S_{co}^{WT} \end{cases} \tag{3}$$

B. Photovoltaic Unit and Beta PDF

In this study, the Beta PDF is selected to model the solar irradiance distribution, as shown in (4) [9]. The shape of the beta density function can vary widely depending on the values of its two parameters, which determine the location and spread of the distribution. I n general, the distribution tends to be skewed towards one end of the range or the other, but it can also be symmetrical or U-shaped depending on the parameter value. Shape parameters (α and β) are calculated according to the expected value and standard deviation, as presented in (5). To achieve the generation of PV units based on the value of solar irradiation, (6) is used [8]. Parameters η^{PV}, A^{PV}, Γ^{PV}, and T^{O}, which are related to characteristics of photovoltaic panels or environmental conditions, denote conversion coefficient, array area, solar irradiance, and temperature.

$$PDF(x) = \frac{\Gamma(\alpha+\beta)}{\Gamma(\alpha)\Gamma(\beta)}x^{\alpha-1}(1-x)^{\beta-1} \tag{4}$$

$$\beta = (1-\mu)\left(\frac{\mu(1-\mu)}{\sigma^2} - 1\right)\ \&\ \alpha = \frac{\mu\beta}{1-\mu} \tag{5}$$

$$P^{PV} = \eta^{PV}A^{PV}\Gamma^{PV}\left(1 - 0.005(T^{O} - 25)\right) \tag{6}$$

C. Electric Demand and Gaussian PDF

The Gaussian density function, also known as normal distribution, is a probability distribution that is often used in statistics and data analysis to model continuous random variables. The shape of the Gaussian density function is bell-shaped and symmetric around its mean value, with the majority of the data clustered around the mean and the tails of the distribution tapering off to zero as they approach positive and negative infinity. Uncertainties of parameters linked to electricity demand and EVs are usually modeled via Gaussian PDF [10].

$$PDF(x) = \frac{1}{\sigma\sqrt{2\pi}}e^{-\frac{(x-\mu)^2}{2\sigma^2}} \tag{7}$$

D. Scenario Generation

Probability density function approximation via scenario generation involves generating a set of scenarios that represent possible outcomes of a random variable. The Gaussian, Beta, and Weibull PDFs are used in this study to generate scenarios for the uncertain parameters. By taking advantage of these scenarios, a two-stage stochastic programming optimization is formulated. For scenario generation, the method that is presented in [11] is deployed. In this approach, the probability (ρ_{x,r_x}) of the set scenarios (r_x) of uncertain parameter (x) is calculated based on (8). Albeit, in [11], only 7 scenarios are generated and considered for uncertain parameters, 13 scenarios are generated in this paper to model uncertainty more accurately.

$$\rho_{x,r_x} = \int_{x_{start}}^{x_{end}} xPDF(x)dx \tag{8}$$

III. Mathematical Formulation

In this section, a mixed-integer second-order cone programming model for the optimal operation of MGs is presented. Then, the MG is rescheduled to improve the resiliency against outages when it is most dependent on the main grid.

A. Two-stage Stochastic Model for Optimal Operation of Microgrids

Stochastic optimization has been widely used in power system studies to model uncertainty; a generic formulation for two-stage stochastic programming is presented in (9). Variables x_1 and x_2 represent a set of decision variables at the first and second stages, respectively. $f(x_1)$ is the part of the objective function linked to the first stage (before realization of uncertainty), while $E\{g(x_1, x_2)\}$ is the second part of the objective function (based on expected value) related to the realization of scenarios.

$$\min_{x_1,x_2} f(x_1) + E\{g(x_1, x_2)\} \tag{9}$$

In (10), the objective function (i.e., total cost minimization) of the optimal operation of the MG is presented, where parameters Γ_{dg}^{a}, Γ_{dg}^{b}, and Γ_{dg}^{c} denote cost coefficients of distributed generation (DG) units. Additionally, variables $P_{dg,t,s}^{DG}$, $P_{t,s}^{GR}$, and $\psi_{m,t,s}^{SHED}$ are the generation of DG units, the power exchanged by the main grid, and the amount of load curtailment. $P_{m,t,s}^{D}$ is the power demand and parameters Γ^{SHED} and $\Gamma_{t,s}^{GR}$ are associated with load curtailment cost and electricity price. The probability of scenarios and time interval are represented by Π_s and Δ_t. Moreover, binary variable $\vartheta_{dg,t}^{DG}$ is defined to model the commitment of DG units in the first stage. The power balance is ensured by including (11) and (12), wherein R_{mn} and X_{mn} represent the resistance and reactance of the line mn. Here, $P_{km,t,s}$ denotes the active power flows through line km (from bus k to m), while $P_{pv,t,s}^{PV}$, $P_{wt,t,s}^{WT}$, $P_{bs,t,s}^{BS}$, and $P_{ev,t,s}^{EV}$ represent the power produced by PV units, power produced by WT units, the charging/discharging power of batteries, and charging power of EVs. In analogous fashion, variables $Q_{km,t,s}$, $Q_{t,s}^{GR}$, $Q_{dg,t,s}^{DG}$, and parameter $Q_{m,t,s}^{D}$ denote the flow of reactive power from bus k to bus m, the reactive power exchanged between the main grid and the MG, the reactive power generated by DG units, and the reactive power demanded by consumers in the MG, respectively. Constraint (13) models the relation between the voltage levels of buses and the active power, reactive power, and current flowing in the lines of the MG. Here, $V_{m,t,s}^{sqr}$ and Z_{mn} represent the square of voltage magnitude at bus m and the impedance of line mn, respectively. Constraint (14) captures the connection between

the current, active power, reactive power, and voltage levels of buses. Additionally, the physical constraints on voltages and currents in the MG are modeled using (15) and (16), in which the upper bound of voltage ($\overline{V}$), the lower bound of voltage ($\underline{V}$), and the upper bound of current ($\overline{I}$) denote the acceptable range of voltages and currents. The technical limitations associated with DG units are taken into account by utilizing equations (17)–(20), where $\underline{P}_{dg}$ and $\overline{P}_{dg}$ denote the lower and upper boundaries for power generated by DG units and φ_{dg}^{DG} indicates the power factor of DG units. Constraints that pertain to the operation of batteries are presented in (21)–(27), where $P_{bs,t,s}^{BS+}$ and $P_{bs,t,s}^{BS-}$ are variables that are non-negative and defined to simulate the charging and discharging power of batteries. Additionally, $\varrho_{bs,t,s}^{+}$ and $\varrho_{bs,t,s}^{-}$ are binary variables defined to prevent simultaneous charging and discharging, as stipulated in equation (24). In (25) and (26), the relation between power and energy of batteries is modeled, while the energy loss in batteries is also included and constraints corresponding to energy capacity of batteries are represented in (27). Parameters $\check{E}_{bs}^{BS}$, η_{bs}^{BS}, β_{bs}^{BS}, $\underline{E}_{bs}$, and $\overline{E}_{bs}$ denote the initial energy, efficiency, self-discharge rate, and the minimum and maximum capacity of batteries. Constraints (28)–(32) are used to represent how EVs function as controllable electric loads in the microgrid (MG) [12]. Additionally, this formulation assumes that each EV has a known initial state-of-charge. The primary objective concerning the EVs is to fulfill the energy requirement, specifically for a trip. Constraint (28) sets the power limit for charging of EVs ($P_{ev,t,s}^{EV}$) by defining the maximum charger power as $\overline{P}_{ev}$. The power for motion attained by each EV relies on its availability state indicated by the binary parameter $\zeta_{ev,t,s}$. This parameter takes on a value of 1 if the EV is accessible for charging and 0 if it is not connected to the MG. The amount of energy stored in the batteries of the EVs during the initial time period of the charging schedule, denoted by (29), is dependent on several factors, including the initial stage of charge ($E_{ev,s}^{Ini}$), the energy required for the EV to travel (E_{ev}^{Trip}), and a binary parameter that indicates whether the EV is currently in use for transportation or not ($C_{ev,t}$). Equation (30) is similar to (29), but is applied to time periods after t_1. Constraint (31) ensures that the amount of energy stored in the battery of EV is greater than the energy required for transportation. Additionally, constraint (32) sets limits on the minimum and maximum amounts of energy can be stored in each battery of EV.

$$min \sum_{dg}\sum_{t} \Gamma_{dg}^{a}\vartheta_{dg,t}^{DG} + \sum_{s} \Pi_s \left(\sum_{t} \Delta_t \Gamma_{t,s}^{GR} P_{t,s}^{GR} + \left(\sum_{dg}\sum_{t} \Delta_t P_{dg,t,s}^{DG} \Gamma_{dg}^{b} + \sum_{\omega} \left(\Delta_t P_{dg,t,s}^{DG}\right)^2 \Gamma_{dg}^{c} \right) + \sum_{m}\sum_{t} \Delta_t P_{m,t,s}^{D} \psi_{m,t,s}^{SHED} \Gamma^{SHED} \right) \quad (10)$$

$$\sum_{km} P_{km,t,s} - \sum_{mn} \left(P_{mn,t,s} + R_{mn} I_{mn,t,s}^{sqr}\right) + P_{t,s}^{GR} + \sum_{dg|b_{dg}=m} P_{dg,t,s}^{DG} + \sum_{pv|b_{pv}=m} P_{pv,t,s}^{PV} + \sum_{wt|b_{wt}=m} P_{wt,t,s}^{WT} = P_{m,t,s}^{D}\left(1 - \psi_{n,t,s}^{SHED}\right) + \sum_{bs|b_{bs}=m} P_{bs,t,s}^{BS} + \sum_{ev|b_{ev}=m} P_{ev,t,s}^{EV}; \ \forall m,t,s \quad (11)$$

$$\sum_{km} Q_{km,t,s} - \sum_{mn} \left(Q_{mn,t,s} + X_{mn} I_{mn,t,s}^{sqr}\right) + Q_{t,s}^{GR} + \sum_{dg|b_{dg}=m} Q_{dg,t,s}^{DG} = Q_{m,t,s}^{D}; \forall m,t,s \quad (12)$$

$$V_{m,t,s}^{sqr} - V_{n,ts}^{sqr} = 2\left(R_{mn}P_{mn,t,s} + X_{mn}Q_{mn,t,s}\right) + Z_{mn}^2 I_{mn,t,s}^{sqr}; \forall mn,t,s \quad (13)$$

$$V_{n,t,s}^{est} I_{mn,t,s}^{sqr} \geq {P_{mn,t,s}}^2 + {Q_{mn,t,s}}^2; \forall mn,t,s \quad (14)$$

$$\underline{V}^2 \leq V_{n,t,s}^{sqr} \leq \overline{V}^2; \ \forall m,t,s \quad (15)$$

$$0 \leq I_{mn,t,s}^{sqr} \leq \overline{I}^2; \ \forall mn,t,s \quad (16)$$

$$P_{dg,t,s}^{DG} \geq \vartheta_{dg,t}^{DG} \underline{P}_{dg}^{DG}; \ \forall dg,t,s \quad (17)$$

$$P_{dg,t,s}^{DG} \leq \vartheta_{dg,t}^{DG} \overline{P}_{dg}^{DG}; \forall dg,t,s \quad (18)$$

$$Q_{dg,t,s}^{DG} \leq P_{dg,t,s}^{DG} \, tan\left(cos^{-1}\left(\varphi_{dg}^{DG}\right)\right); \ \forall dg,t,s \quad (19)$$

$$Q_{dg,t,s}^{DG} \geq -P_{dg,t,s}^{DG} \, tan\left(cos^{-1}\left(\varphi_{dg}^{DG}\right)\right); \forall dg,t,s \quad (20)$$

$$0 \leq P_{bs,t,s}^{BS+} \leq \overline{P}_{bs}^{BS} \varrho_{bs,t,s}^{+}; \ \forall bs,t,s \quad (21)$$

$$0 \leq P_{bs,t,s}^{BS-} \leq \overline{P}_{bs}^{BS} \varrho_{bs,t,s}^{-}; \ \forall bs,t,s \quad (22)$$

$$P_{bs,t,s}^{BS} = P_{bs,t,s}^{BS+} - P_{bs,t,s}^{BS-}; \ \forall bs,t,s \quad (23)$$

$$\varrho_{bs,t,s}^{+} + \varrho_{bs,t,s}^{-} \leq 1; \ \forall bs,t,s \quad (24)$$

$$E_{bs,t,s}^{BS} = \check{E}_{bs}^{BS} + \Delta t \left(P_{bs,t,s}^{BS+} \eta_{bs}^{BS} - \frac{P_{bs,t,s}^{BS-}}{\eta_{bs}^{BS}} - E_{bs,t,s}^{BS} \beta_{bs}^{BS} \right); \forall bs,t,s|t = 1 \quad (25)$$

$$E_{bs,t,s}^{BS} = E_{bs,t,s}^{BS} + \Delta t \left(P_{bs,t,s}^{BS+} \eta_{bs}^{BS} - \frac{P_{bs,t,s}^{BS-}}{\eta_{bs}^{BS}} - E_{bs,t,s}^{BS} \beta_{bs}^{BS} \right); \forall bs,t,s|t \geq 1 \quad (26)$$

$$\underline{E}_{bs} \leq E_{bs,t,s}^{BS} \leq \overline{E}_{bs}; \ \forall bs,t,s \quad (27)$$

$$0 \leq P_{ev,t,s}^{EV} \leq \zeta_{ev,t,s} \overline{P}_{ev}; \ \forall ev,t,s \quad (28)$$

$$E_{ev,t,s}^{EV} = E_{ev,s}^{Ini} + P_{ev,t,s}^{EV} \Delta t_t - E_{ev}^{Trip} \frac{C_{ev,t}}{\sum_{k \in T} C_{ev,k}}; \forall ev,t,s|t = t_1 \quad (29)$$

$$E_{ev,t,s}^{EV} = E_{ev,t-1,s}^{EV} + P_{ev,t,s}^{EV} \Delta t_t - E_{ev}^{Trip} \frac{C_{ev,t}}{\sum_{k \in T} C_{ev,k}}; \forall ev,t,s|t \geq t_1 \quad (30)$$

$$E_{ev,t,s}^{EV} \geq E_{ev}^{Trip} \frac{C_{ev,t}}{\sum_{k \in T} C_{ev,k}}; \forall ev,t,s \quad (31)$$

$$\underline{E}_{ev}^{EV} \leq E_{ev,t,s}^{EV} \leq \overline{E}_{ev}^{EV}; \forall ev,t,s \quad (32)$$

B. Outage Modeling and Scenario Selection

The islanding of the MG can be modeled by adding (33) and (34) to the normal operation model [6]. In this study, the time interval when the MG receives the maximum amount of power from the main grid during the time horizon is selected as a plausible outage interval (t^*) to be used for rescheduling purpose.

$$P_{t,s}^{GR} = 0; \quad \forall t,s|t = t^* \quad (33)$$

$$Q_{t,s}^{GR} = 0; \quad \forall t,s|t = t^* \quad (34)$$

The steps of the proposed method are summarized as a flowchart and depicted in Fig. 1. In this approach, firstly the developed model is solved to find the best solutions for the scheduling of the MG. Then, the time intervals when the MG imports the largest amount of power from the main grid is determined. The MG is rescheduled based on the assumption that the unplanned outages will happen during this time interval, so preventive actions can be done in the first stage to mitigate the damaging consequences. In other words, the commitment of DG units decisions can be modified to avoid costly consequences of unplanned islanding.

IV. Test and Results

To evaluate the proposed resilient-oriented model for the optimal operation of the MGs, a modified IEEE 33-bus network consisting of wind turbines, photovoltaic units, batteries, distributed generation units, and charging stations is considered (shown in Fig. 2). The realizations for electric load, solar irradiation, wind speed, and electricity price are illustrated in Fig. 3–Fig. 6. The data on MG components is presented in Table I and Table II. The proposed models were developed in AMPL and solved by CPLEX [13] in a computer with an Intel i5-1135G7 processor and 16 GB of RAM.

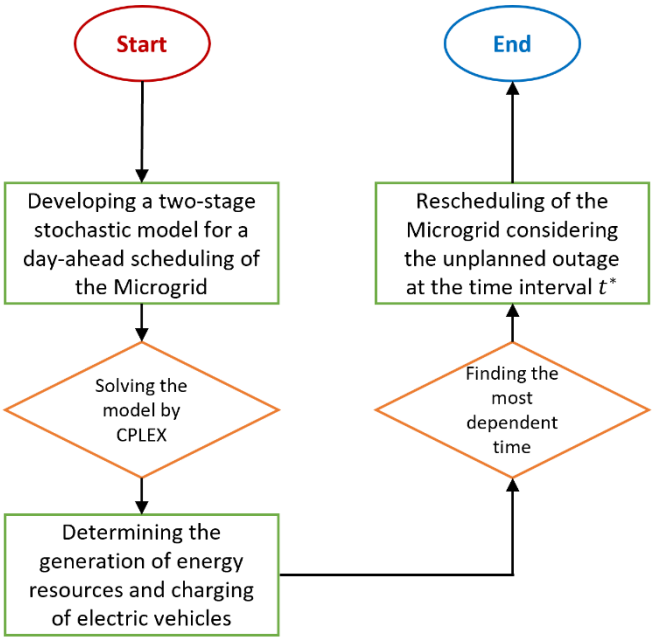

Fig. 1. Flowchart of the proposed approach for resilient optimal operation of microgrids.

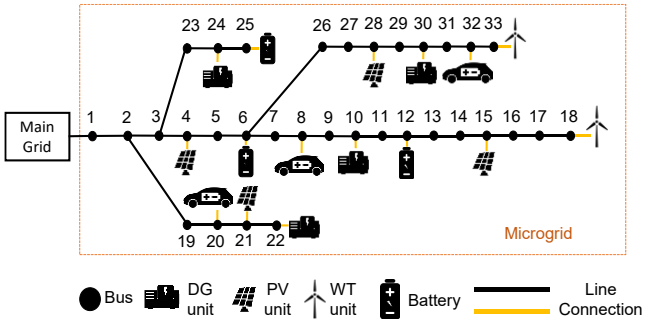

Fig. 2. Diagram of the 33-bus test system.

TABLE I. PARAMETERS OF DISTRIBUTED GENERATION UNITS

Characteristic	DG unit 1	DG unit 2	DG unit 3
Bus	10	22	24
$\overline{P}_{dg}^{DG}$(kW)	500	750	750
$\underline{P}_{dg}^{DG}$(kW)	50	100	100
φ_{dg}	1.0	0.8	0.9
a_{dg}($)	27	25	26
b_{dg}($/MWh)	87	87	81
c_{dg}($/MWh^2)	0.0025	0.0035	0.185

TABLE II. PARAMETERS OF BATTERIES

Characteristic	Battery 1	Battery 2	Battery 3
Bus	6	12	25
$\overline{S}_{bs}^{BS}$(kW)	200	200	100
$\overline{E}_{bs}^{BS}$(kWh)	1200	1000	800
$\underline{E}_{bs}^{BS}$(kWh)	200	150	100
η_{bs}^{Ch} & η_{bs}^{Dis}	0.95	0.85	0.90
β_{bs}	0.002	0.002	0.004

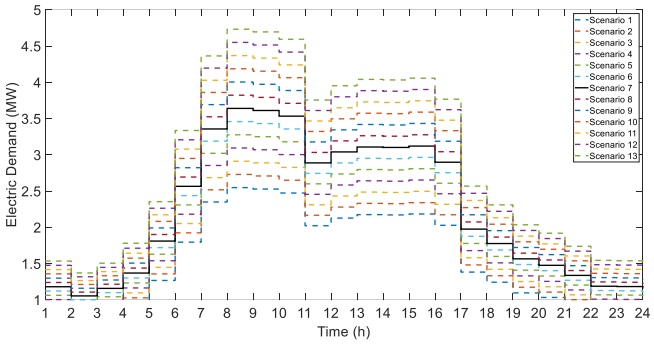

Fig. 3. Scenarios for power demand.

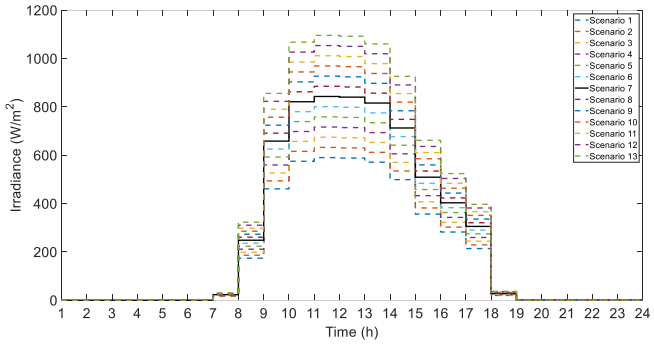

Fig. 4. Scenarios for solar irradiation.

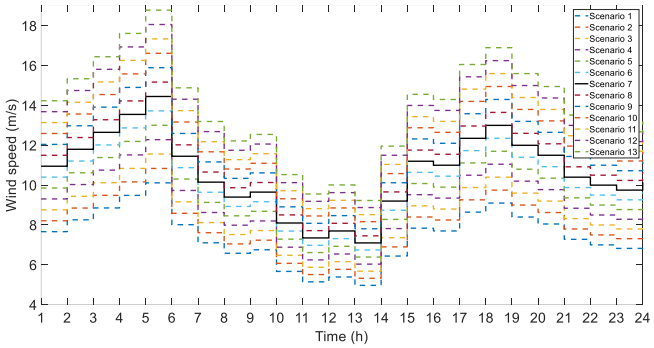

Fig. 5. Scenarios for wind speed.

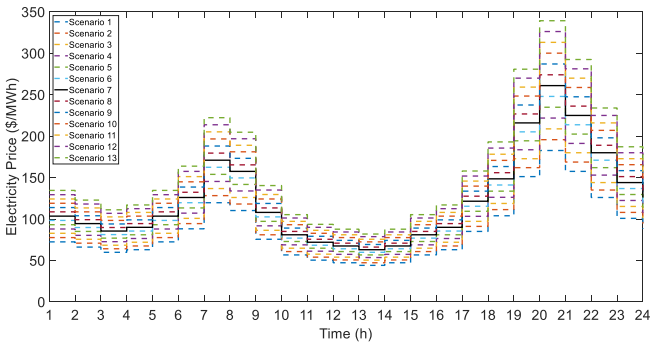

Fig. 6. Scenarios for electricity price.

A. Case I: Two-stage Stochastic Without Any Outage Occurrence

In this case study, the two-stage stochastic model for the optimal operation of MG without any outages is solved. It is worth mentioning that commitment of DG units and charging of EVs are considered here-and-now decisions. The obtained operation cost of the MG was $1959.82. The average, maximum, and minimum power exchanged between the MG

and the main grid are depicted in Fig. 7, illustrating that the MG buys the power from the grid before $t = 16$ and sells the power to the grid from $t = 17$ to $t = 24$.

Moreover, the maximum power is bought from the main grid at $t = 13$, which is around 2500 kW. The average generation of DG units and charging (discharging) of batteries are visualized in Fig. 8. According to Fig. 8, DG units generate active power between $t = 6$ and $t = 8$ in the morning and from $t = 17$ and $t = 23$ in the afternoon and evening, showing that at least one of the DG units generates power during this 10-hour time period. The charging of EVs is presented in Fig. 9, showing that the maximum charging occurs at $t = 12$ and $t = 13$.

B. Case II: Two-stage Stochastic Including Outage Without Preventive Actions

This subsection presents the results associated with the proposed two-stage stochastic programming model for the optimal operation of MGs considering smart charging; while (33) and (34) are included to model outages, no preventive actions have been considered. As a result, the commitment of DG units (here-and-now decision) is fixed to the solutions obtained from Case I. The total cost of MG is obtained \$2559.6, indicating 30.60% increase in the cost due to outages at $t = 12$ and $t = 13$. In other words, if the operators only schedule the MG based on the optimal solution achieved in the Case I and outages occurs at the aforementioned time intervals, the total cost of the MG can increase significantly.

In Fig. 10, the average, maximum, and minimum power exchanged between the MG and the main grid is depicted. It can be seen that no power is exchanged at $t = 12$ and $t = 13$, so outages are modeled successfully. Furthermore, comparing Fig. 7 and Fig. 10 shows some changes in the power exchanges. In Fig. 11, the scheduling of DG units and batteries is depicted. According to Fig. 11, DG 1 and DG 2 as well as Battery 3 (BS 3) compensate the power shortage due to islanding by injecting power to the MG. The charging of EVs is shown in Fig. 12.

C. Case III: The Proposed Resiliency-oriented Model

In this case, the model is solved while the resiliency of the MG is enhanced to reinforce the solution against outages at time intervals $t = 12$ and $t = 13$. In other words, equations (10)–(34) are included and the optimal solution is achieved with a cost of \$2141.84, showing 16.32% reduction in the cost of the MG compared to Case II. As a result, the proposed model can reduce the cost of MG by adopting preventive actions in the first-stage decision procedure. Similar to Case I and Case II, in Fig. 13, the average, maximum, and minimum power exchanged between the MG and the main grid are visualized. On one hand, by comparing Fig. 10 and Fig. 13, it can be noticed that the MG buys more power from the main grid in Case III compared to Case II.

On the other hand, the scheduling for DG units and batteries is depicted in Fig. 14, which indicates that less DG generation is needed in Case III in comparison to Case II. In addition, the pattern for charging and discharging of EVs also has changed to minimize the costly consequences of the unplanned islanding at the respective time intervals, as shown in Fig. 15. It can be seen in Fig. 15, that the charging of EVs have shifted to left, so EVs charge mainly between $t = 9$ and $t = 11$ in comparison to Case I and Case II, in which the charging has principally done from $t = 9$ to $t = 11$.

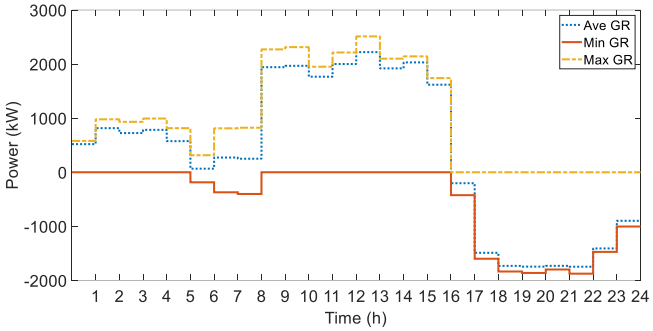

Fig. 7. Power exchanged between the main grid and microgrid in Case I.

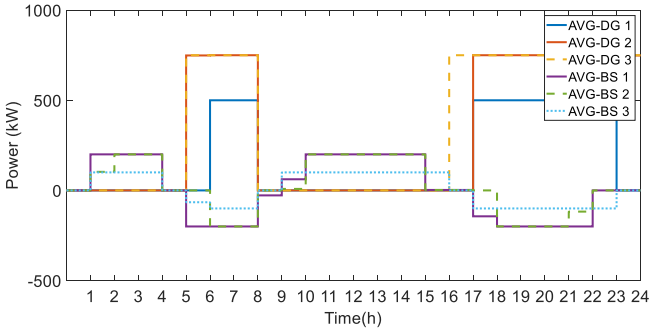

Fig. 8. Scheduling of DG units and batteries in Case I.

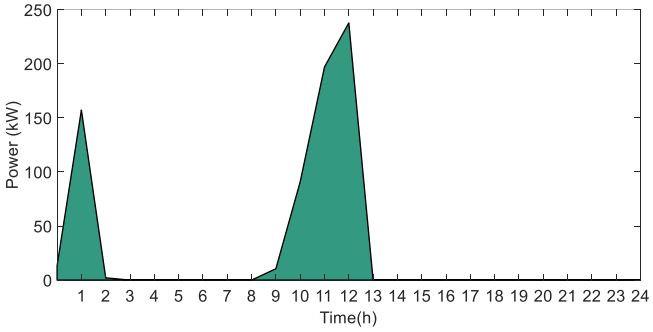

Fig. 9. Charging of EVs in Case I.

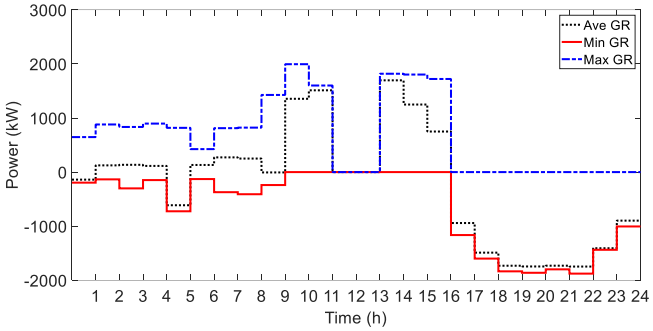

Fig. 10. Power exchange between the main grid and microgrid in Case II.

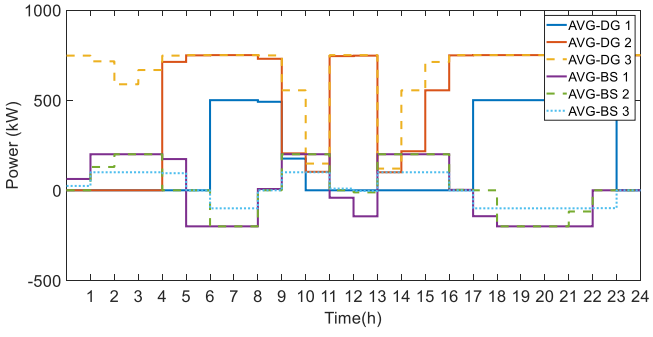

Fig. 11. Scheduling of DG units and batteries in Case II.

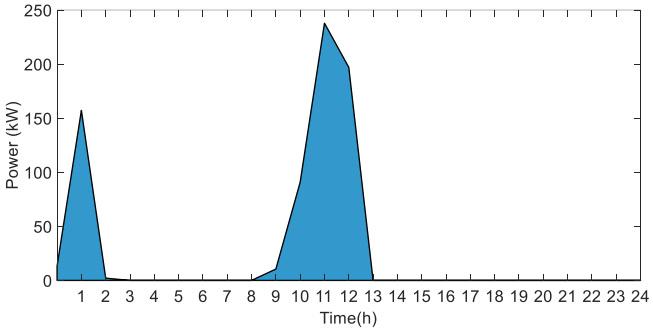

Fig. 12. Charging of EVs in Case II.

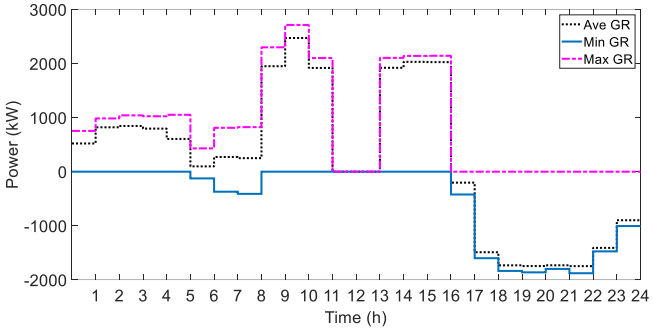

Fig. 13. Power exchange between the main grid and microgrid in Case III.

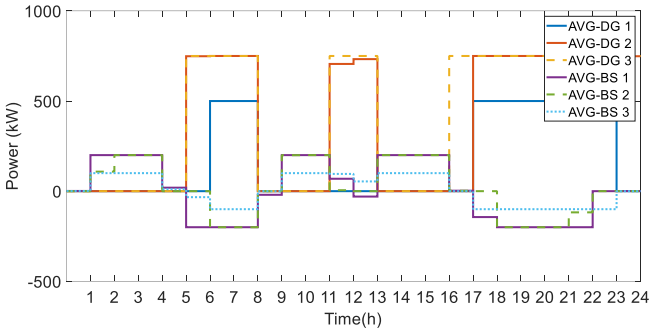

Fig. 14. Scheduling of DG units and batteries in Case III.

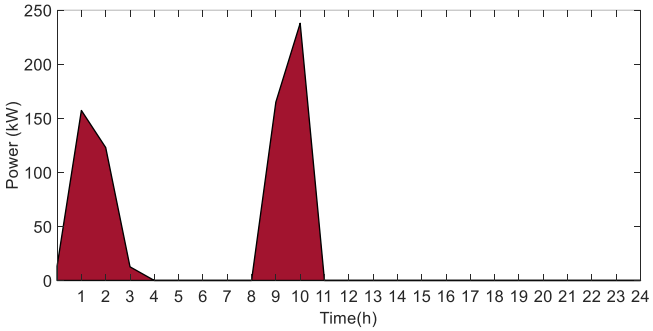

Fig. 15. Charging of EVs in Case III.

V. Conclusion

Microgrids (MGs), self-contained power systems, can incorporate renewable energy sources, such as solar and wind power, at a smaller scale. This allows for greater energy independence and reduces the reliance on non-renewable sources. Similarly, electric vehicles (EVs) help to reduce emissions by using electricity instead of gasoline or diesel fuel. When powered by renewable energy sources, EVs can significantly reduce greenhouse gas emissions, improve air quality, and decrease dependence on fossil fuels. However, it is essential to address uncertainty and resiliency issues to guarantee the validity of solutions and resilient operations during unplanned outages. Hence, a two-stage stochastic programming model that aims to ensure the resiliency of MGs has been proposed. The model considers uncertainties related to renewable energy generation, market prices, and power demand by employing multiple scenarios. To improve MG resilience, a scenario involving outages is included. This allows preemptive measures to be taken in the first stage to reinforce the energy management system against unforeseen power outages. The results showed that the total cost of the MG can be reduced by 16.32% by the proposed method compared to the indiscriminate scheduling, where likely outages are neglected. This research assumes that EVs can function as controllable loads without considering vehicle-to-grid technology. Additionally, the presented power flow formulation is appropriate for balanced MGs. Consequently, future work may explore EV charging stations with vehicle-to-grid capabilities and adapt the proposed model to accommodate unbalanced MGs.

References

[1] L. Hou, J. Dong, O. E. Herrera, and W. Mérida, “Energy management for solar-hydrogen microgrids with vehicle-to-grid and power-to-gas transactions,” Int. J. Hydrogen Energy, vol. 48, no. 5, pp. 2013–2029, 2023.

[2] X. Yao, Y. Fan, F. Zhao, and S.-C. Ma, “Economic and climate benefits of vehicle-to-grid for low-carbon transitions of power systems: A case study of China’s 2030 renewable energy target,” J. Clean. Prod., vol. 330, p. 129833, 2022.

[3] S. L. Chartier, V. K. Venkiteswaran, S. S. Rangarajan, E. R. Collins, and T. Senjyu, “Microgrid Emergence, Integration, and Influence on the Future Energy Generation Equilibrium—A Review,” Electronics, vol. 11, no. 5, p. 791, 2022.

[4] M. R. Ebrahimi and N. Amjady, “Adaptive robust optimization framework for day-ahead microgrid scheduling,” Int. J. Electr. Power Energy Syst., vol. 107, pp. 213–223, 2019.

[5] F. Liu, Q. Mo, and X. Zhao, “Two-level optimal scheduling method for a renewable microgrid considering charging performances of heat pump with thermal storages,” Renew. Energy, vol. 203, pp. 102–112, 2023.

[6] J. A. A. Silva, J. C. López, N. B. Arias, M. J. Rider, and L. C. P. da Silva, “An optimal stochastic energy management system for resilient microgrids,” Appl. Energy, vol. 300, p. 117435, 2021.

[7] M. Ebrahimi and A. Sheikhi, “A local integrated electricity-heat market design among multi Smart Energy Hubs with renewable energy generation uncertainty,” Electr. Power Syst. Res., vol. 218, p. 109217, 2023.

[8] H. Karimi, G. B. Gharehpetian, R. Ahmadiahangar, and A. Rosin, “Optimal energy management of grid-connected multi-microgrid systems considering demand-side flexibility: A two-stage multi-objective approach,” Electr. Power Syst. Res., vol. 214, p. 108902, 2023.

[9] H. Karimi, S. Jadid, and A. Makui, “Stochastic energy scheduling of multi-microgrid systems considering independence performance index and energy storage systems,” J. Energy Storage, vol. 33, p. 102083, 2021.

[10] R. Wang, P. Li, H. Yu, H. Ji, W. Xi, and C. Wang, “Identification of critical uncertain factors of distribution networks with high penetration of photovoltaics and electric vehicles,” Appl. Energy, vol. 329, p. 120260, 2023.

[11] H. Karimi and S. Jadid, “Optimal energy management for multi-microgrid considering demand response programs: A stochastic multi-objective framework,” Energy, vol. 195, p. 116992, 2020.

[12] S. F. Zandrazavi, C. P. Guzman, A. T. Pozos, J. Quiros-Tortos, and J. F. Franco, “Stochastic multi-objective optimal energy management of grid-connected unbalanced microgrids with renewable energy generation and plug-in electric vehicles,” Energy, vol. 241, p. 122884, 2022.

[13] I. ILOG, “AMPL CPLEX System Version 11 User’s Guide,” ILOG CPLEX Div., 2008.